Margin-to-Margin Seafloor Spreading in the Eastern Gulf of Aden: A 16 Ma-Long History of Deformation and Magmatism from Seismic Reflection, Gravity and Magnetic Data

Morgane Gillard, Sylvie Leroy, Mathilde Cannat, Heather Sloan

frontiers in Earth Science

ORIGINAL RESEARCH
published: 22 July 2021
doi: 10.3389/feart.2021.707721

Margin-to-Margin Seafloor Spreading in the Eastern Gulf of Aden: A 16 Ma-Long History of Deformation and Magmatism from Seismic Reflection, Gravity and Magnetic Data

Morgane Gillard[1], *Sylvie Leroy*[1]*, *Mathilde Cannat*[2] *and Heather Sloan*[3]

[1]Sorbonne Université, CNRS-INSU, Institut des Sciences de la Terre Paris, F-75005, Paris, France, [2]Marine Geosciences, Institut de Physique du Globe de Paris, UMR 7154, CNRS, Université de Paris, F-75005, Paris, France, [3]Lehman College, City University of New York, Bronx, NY, United States

In this paper we present and analyze spreading-parallel seismic transects that image the oceanic crust in the eastern Gulf of Aden, from the Oman to the Socotra margins, across the active Sheba mid-oceanic ridge and between the Socotra-Hadbeen and Eastern Gulf of Aden Fracture Zones. The correlation of potential field data sets and gravity modelling allow us to document the spreading history of this oceanic basin from the onset of seafloor spreading ~16 Ma-ago to the present. Two main oceanic sub-domains display distinct structural characteristics associated with different magmatic budgets at this mid-ocean ridge. In addition, we document the occurrence of a magmatic pulse at the Sheba Ridge around 11 Ma leading to the construction of a magmatic plateau in the western part of the studied area. This event led to substantial deformation and additional magmatism in previously formed oceanic crust. It could be related to an off-axis magmatic event previously identified in the adjacent Sheba segment, itself possibly related to the Afar plume.

Keywords: oceanic spreading, gulf of aden, seismic reflection, magmatism, sheba ridge

OPEN ACCESS

Edited by:
Nico Augustin,
GEOMAR Helmholtz Center for Ocean Research Kiel, Germany

Reviewed by:
Laurent Gernigon,
Geological Survey of Norway, Norway
Chun-Feng Li,
Zhejiang University, China

***Correspondence:**
Sylvie Leroy
sylvie.leroy@sorbonne-universite.fr,
http://sylvie.leroy@sorbonne-universite.fr/

Specialty section:
This article was submitted to Structural Geology and Tectonics, a section of the journal Frontiers in Earth Science

Received: *10 May 2021*
Accepted: *09 July 2021*
Published: *22 July 2021*

Citation:
Gillard M, Leroy S, Cannat M and Sloan H (2021) Margin-to-Margin Seafloor Spreading in the Eastern Gulf of Aden: A 16 Ma-Long History of Deformation and Magmatism from Seismic Reflection, Gravity and Magnetic Data. Front. Earth Sci. 9:707721. doi: 10.3389/feart.2021.707721

INTRODUCTION

Rifted margins, in particular the transition between continental and oceanic crusts, as well as mid-oceanic ridges, represent two foci of interest for the scientific community. The Eastern Gulf of Aden region offers an opportunity to explore both domains and the intervening oceanic plates in a single survey. In this paper, we present previously unpublished, margin-to-margin seismic transects (ENCENS and MARGES-ADEN surveys) across the eastern Gulf of Aden, between the Socotra-Hadbeen Fracture Zone and the Eastern Gulf of Aden Fracture Zone (the Socotra-Sharbithat segment; **Figure 1A**). For the first time in the history of oceanic basin analysis, we have the opportunity to image a whole oceanic basin and to study each phase of the evolution of conjugate ridge flanks from the onset of seafloor spreading to the present-day mature mid-oceanic ridge. This is new in comparison with previous studies (e.g. Franke, 2013; Tugend et al., 2018) which only focused on a specific domain or restricted area. The Eastern Gulf of Aden is imaged from the northern Oman margin, across the active Sheba mid-oceanic ridge, to the conjugate southern Socotra margin (**Figure 1B**). Each of the seven seismic transects images more than 400 km of oceanic basement and

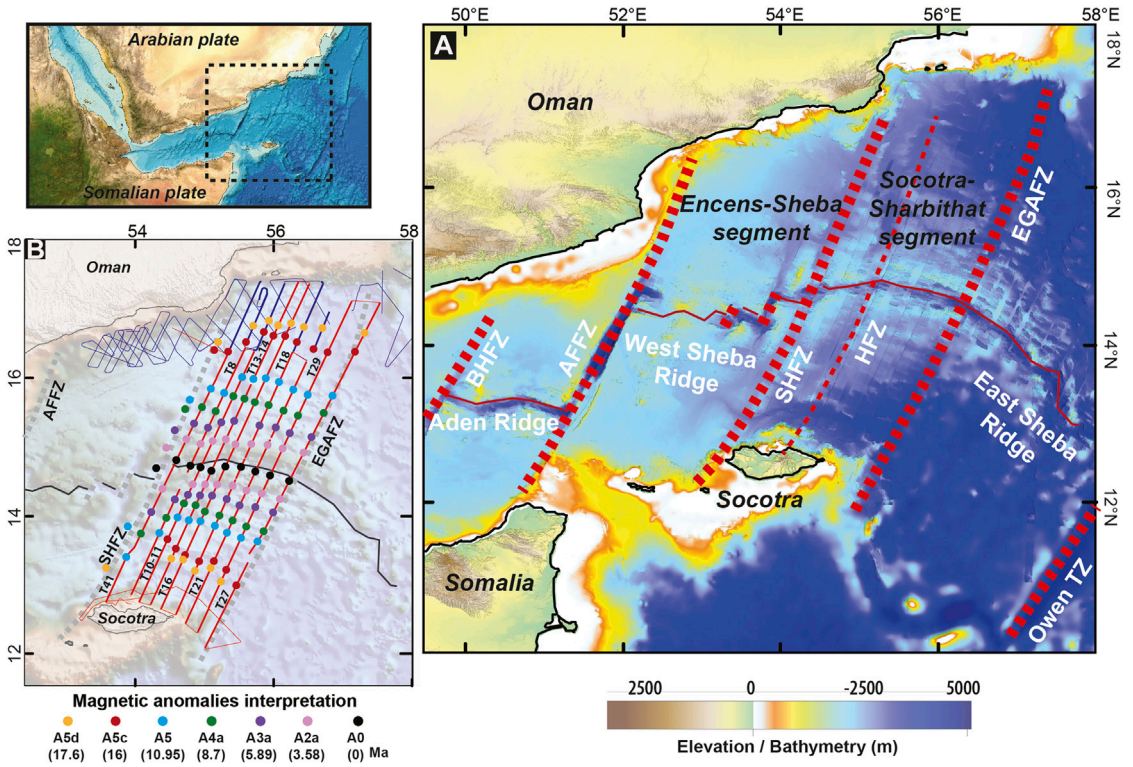

FIGURE 1 | (A) Bathymetric map (GEBCO) showing the studied location with the main fracture zones. BHFZ, Bosaso Hami Fracture Zone; AFFZ, Alula-Fartak Fracture Zone; SHFZ, Socotra-Hadbeen Fracture Zone; HFZ, Hadibo Fracture Zone (this paper); EGAFZ, Eastern Gulf of Aden Fracture Zone; Owen TZ, Owen Transform Zone. In thin red the ridge axis. **(B)** Location of the ENCENS survey seismic lines (in blue) and Marges-Aden (MAD) survey (in red) associated with the interpreted magnetic anomalies. Thick lines represent the transects used in this study, thin lines represent the other available seismic data.

is associated with gravity and magnetic data to reveal the evolution and variability of the oceanic basement topography and architecture, from seafloor spreading initiation 16 Ma ago to the current spreading mid-oceanic ridge. Current spreading rates in the Gulf of Aden increase from west to east, from 15.5 mm/year (full rate) for the Aden Ridge, to 22.7 mm/year (full rate) for the East Sheba Ridge (Fournier et al., 2001; Leroy et al., 2010b). These values place the ridges of the Gulf of Aden at the limit between slow and ultra-slow spreading centers (Dick et al., 2003). Variations in the magmatic supply and thus in the spreading mode, have been observed in similar ultra-slow spreading, along different segments of the Southwest Indian Ridge (e.g., Cannat et al., 2003). In the studied Socotra-Sharbithat segment, the density of available seismic transects allows us to refine the segmentation of the ridge, identify spreading asymmetries and to discuss if melt supply variations are similar to those along the Sheba Ridge. But what about variations through time? The seismic data presented in this paper covers 16 Ma of spreading history in this basin and one aim of this paper is thus to determine if the spreading mode is stable or, on the contrary, varies through time. Can we observe a magmatic evolution of the spreading center between the early stage, when the asthenospheric mantle rose against the continental margin, and more mature stage?

One particularity of the Gulf of Aden is the proximity of the Afar mantle plume. It is inferred that the Afar plume had a direct influence on rifting in the western part of the Gulf (from the Gulf of Tadjoura to the Xiis-Al-Mukalla fracture zone), where volcanic activity of Afar mantle plume induced the development of volcanic rifted margins. East of the Xiis-Al-Mukalla fracture zone (XAMFZ), the margins are considered as hybrid (Nonn et al., 2019), i.e. involving a combination of mantle exhumation and significant magmatic supply. East of Alula-Fartak Fracture zone (AFFZ; **Figure 1A**), they are considered magma-poor. The Afar plume is nonetheless proposed to have influenced the localization of continental breakup in this eastern region (Hopper et al., 1992; Buck, 2004; Leroy et al., 2012; Bellahsen et al., 2013), with the channeling of magmatic material from the Afar mantle plume along the developing ocean-continent transition zone (OCT) through the AFFZ (Leroy et al., 2010a). This influence of plume-ridge interaction could persist to present day in the Encens-Sheba segment of the Gulf of Aden (**Figure 1A**), manifested as recent off-axis volcanism (Leroy et al., 2010b). Could the Afar mantle plume have similarly

influenced or affected the magmatic supply in the most eastern segment of the Gulf of Aden, specifically to the Socotra-Sharbithat segment? To address these questions, we combine interpretation of several seismic reflection transects with bathymetric, gravity and magnetic data. We investigate the crustal architecture and characteristics of the oceanic basement from the Oman margin to its conjugate, the southern Socotra margin. This leads us to identify and map different oceanic domains and asymmetries and to discuss how tectonic and magmatic plate divergence processes evolved in the Socotra-Sharbithat segment.

GEOLOGICAL SETTING

The Gulf of Aden extends over 1,400 km between the Indian Ocean and the Afar plume. In the central and eastern part of the Gulf, continental rifting began during the Oligocene, around 34 Ma (Watchorn et al., 1998; Leroy et al., 2012). To the east of the AFFZ (**Figure 1**), the end of the rifting phase was marked by the development of a magma-poor OCT, with supposed mantle exhumation around 20 Ma (Leroy et al., 2004, 2010a; Autin et al., 2010; Nonn et al., 2017). This hypothesis is based on seismic interpretation and particularly on the observation of intra-basement reflections and sedimentary architectures which highlight the continental crust termination and the downlap of sediments over a new basement. Seafloor spreading initiated soon after, splitting old oceanic lithosphere to the east of the Ras Sharbithat and Socotra Island (Stein and Cochran, 1985; Fournier et al., 2010) and leading to the development of the East Sheba Ridge (**Figure 1A**). Further to the west, rifting of continental domains at 17.6 Ma resulted in the nearly synchronous formation of the West Sheba and Aden Ridges (**Figure 1A**) (d' Acremont et al., 2006, 2010; Leroy et al., 2012). The current ridge axis is segmented by several transform faults that trend NNE-SSW (**Figure 1A**), parallel to spreading, defining several segments. The opening direction between Arabian and African plates is therefore oblique to the general ENE-WSW trend of the Gulf of Aden.

This study focuses on the Socotra-Sharbithat segment, bounded by the SHFZ to the west and by the EGAFZ to the east (**Figure 1**). The development of the conjugate margins (Socotra Island to the south and Dhofar margin to the north) is associated with uplift and late tilting (Leroy et al., 2012; Pik et al., 2013; Robinet et al., 2013). These events are recorded in the syn-rift sedimentary sequence which is characterized by the presence of conglomeratic fan-deltas and reef carbonates (Leroy et al., 2012). On the south Socotra margin, the continental breakup of the Neoproterozoic basement resulted in distinct eastern and western structural domains, separated by the NE-SW Hadibo Transfer Zone (Leroy et al., 2012; Bellahsen et al., 2013). This transfer zone represents a pre-existing structure associated with Permian-Triassic rifting which was reactivated during the opening of the Gulf of Aden (Pik et al., 2013).

In the Socotra-Sharbithat segment, the OCT domain, or transition between the continental margin and the first, unambiguous oceanic crust (i.e. formed at a mature spreading center), has been studied by Nonn et al. (2017). They propose that mantle exhumation occurred along one or several detachment faults during the evolution of this domain and that this exhumation phase was associated with notable volcanism. Nonn et al. (2017) defined the transition with the first oceanic crust by the onset of a more volcanically active period, with volcanic units downlapping or onlapping on the exhumed mantle domains. This transition is also associated with the disappearance of the syn-OCT sedimentary units and with the occurrence of well-defined magnetic anomalies (**Figure 1B**).

DATA SETS AND METHODS

Seismic reflection data discussed here were acquired during the ENCENS and MARGES-ADEN (MAD) surveys. The ENCENS multi-channel (360 traces spaced at 12.5 m) seismic reflection survey (Leroy, 2006; Leroy et al., 2010a), focused on the offshore region of Oman (**Figure 1B**). The data were acquired using a single bubble type source of 14 air guns (1.3 L). Previous papers using these data focused on the architecture and development of the OCT (Lucazeau et al., 2008, 2009, 2010; Autin et al., 2010; Leroy et al., 2010a; Watremez et al., 2011; Nonn et al., 2017). The acquisition parameters allow for a good penetration and the imaging of deep structures in the crust. The trade-off for higher resolution of deep crustal structure in this survey is poorer resolution of shallower basement and sediments. The MAD survey (Leroy, 2012; Nonn et al., 2017) acquired margin-to-margin multi-channel (24 traces spaced at 12.5 m) seismic reflection transects, cross-cutting the spreading axis. Multibeam bathymetric and magnetic data were acquired along the same transects. The survey is located in the Socotra-Sharbithat segment (**Figure 1B**). The acquisition parameters for the MAD seismic survey (SN408 Laboratory, SERCEL digital technology) allowed for a high resolution of the shallow basement and sediments but a low penetration in the crust. Previously published papers using these data focused on the near-shore part of the lines imaging the OCT (Leroy et al., 2012; Nonn et al., 2017). In this paper, we focus on the unpublished, oceanic part of the ENCENS and MAD seismic lines, from the OCT to the spreading axis. The seismic lines have been processed by filtering, Normal Move-Out (NMO), stack and migration (Leroy et al., 2010a; Autin et al., 2010). We merged the processed seismic lines from both cruises into seven margin-to-margin transects (**Figure 2**).

For the location of the OCT (**Figures 2**, **3**) we mainly refer to Nonn et al. (2017) as our own criteria to locate the OCT are the same: disappearance of the syn-OCT sedimentary units, volcanic units downlapping or onlapping on the proposed exhumed mantle domains and occurrence of well-defined magnetic anomalies. However, for the three easternmost seismic transects (T21, T29 and T27), Nonn et al. (2017) have changed their methodology and have based their OCT location on heat flow measurements (a "stable" value at about 120 mWm-2) that are well-correlated with the identified A5d magnetic anomaly (Lucazeau et al., 2010). We decided to use a coherent approach for the entire segment, adhering to our criteria

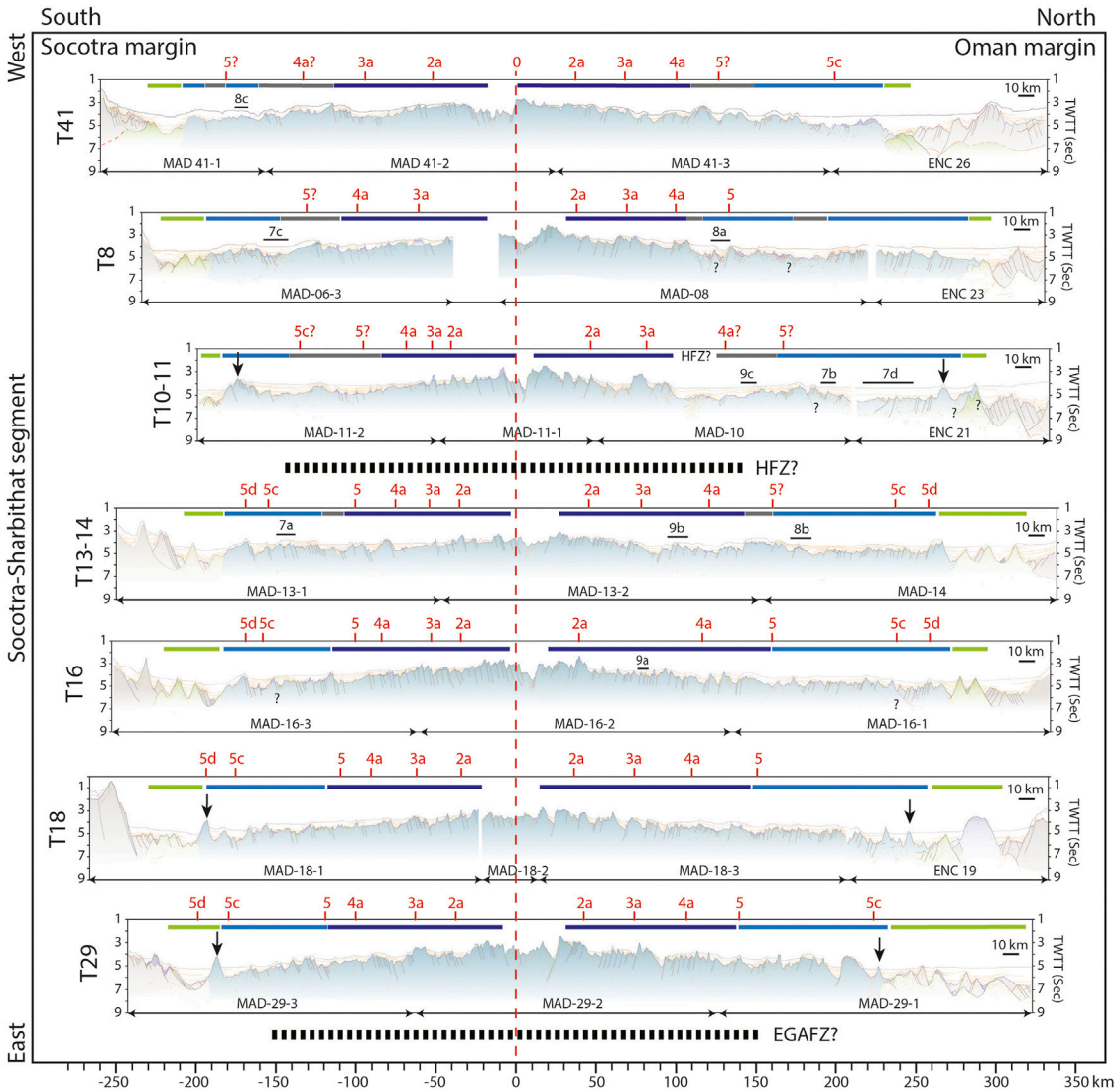

FIGURE 2 | Interpreted seismic transects along the Socotra-Sharbithat segment, in two-ways travel time (TWTT, seconds). Transects T21 and T27 are too noisy and not displayed. The transects are aligned on the magnetic anomaly 0 (ridge axis). The other interpreted magnetic anomalies are displayed in red. In green the OCT domain, in light blue the old oceanic domain (in grey the smooth and regular basement subdomain), in dark blue the young oceanic domain. Black arrays locate the basement ridge associated with the end of the OCT/first oceanic crust. Close up locations shown in **Figures 6**,**7**,**8** are indicated by figure number on each transect. The dashed dark lines between transects represent the fracture zones (HFZ: Hadibo Fracture Zone, EGAFZ: Eastern Gulf of Aden Fracture Zone).

based on stratigraphy and structural observations on the seismic sections. As a consequence, our OCT for the three eastern transects is defined slightly toward the south for the northern margin compared to that of Nonn et al. (2017), which follows the A5d magnetic anomaly.

Multibeam bathymetry and magnetic data were also acquired during the ENCENS and ENCENS-FLUX surveys (Leroy, 2006, Lucazeau and Leroy, 2006; Leroy et al., 2010a; Nonn et al., 2017). The magnetic anomaly identifications are made by comparing each magnetic anomaly profile with a synthetic 2-D block model (**Figure 4**). The synthetic model calculation uses the magnetic reversal timescale modified from Cande and Kent (1995) by Patriat et al. (2008). Although more recent magnetic reversal timescales have appeared in the literature (e.g., Ogg et al., 2020), these later timescales include no significant modifications to anomalies younger than A6 which is older than seafloor within the study area. The model calculation was adapted for slow spreading ridges and took into account the location and orientation of the transects. The synthetic anomaly forms correspond well with the easily recognizable magnetic anomaly sequences in the transect profiles making it possible to identify the full sequence 2a (3.58 Ma), 3a (5.89 Ma), 4a (8.7 Ma), 5 (10.95 Ma), 5c (16 Ma), and 5 days (17.6 Ma) in almost all transects.

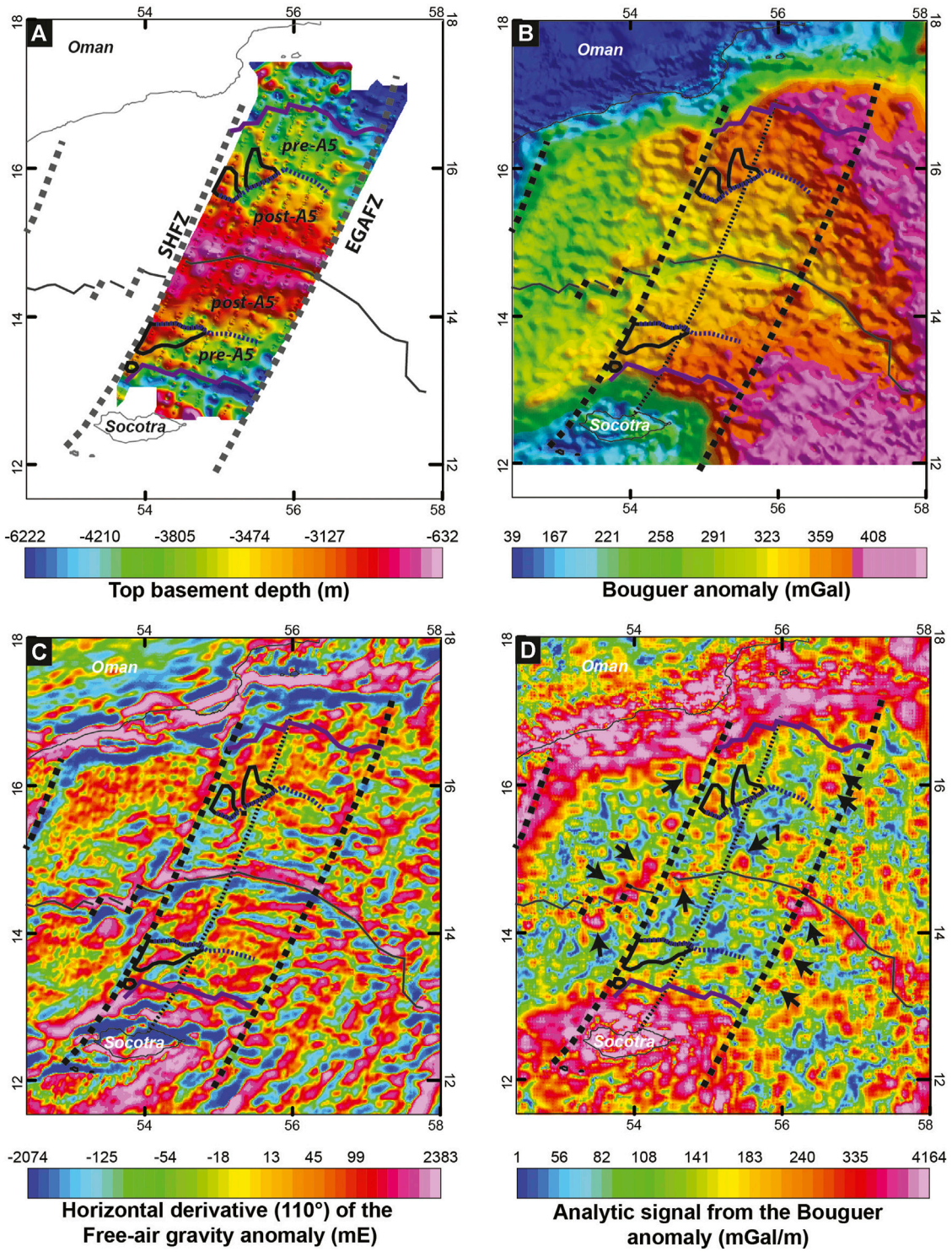

FIGURE 3 | (A) Top basement depth map from seismic profiles; **(B)** Bouguer anomaly map; **(C)** First horizontal derivative of the free-air gravity anomaly map (from Sandwell and Smith, 2009); **(D)** Analytic signal calculated on the Bouguer anomaly map. Arrows point to patches of high Bouguer anomaly values. Thin dotted black line represents the area of thin oceanic crust interpreted as the Hadibo Fracture Zone (see the discussion). OCT termination shown in thick violet (modified from Nonn et al., 2017). Thick doted lines are the known fracture zones (SHFZ and EGAFZ). Areas outlined in black represent the smooth and regular basement subdomain described in the text.

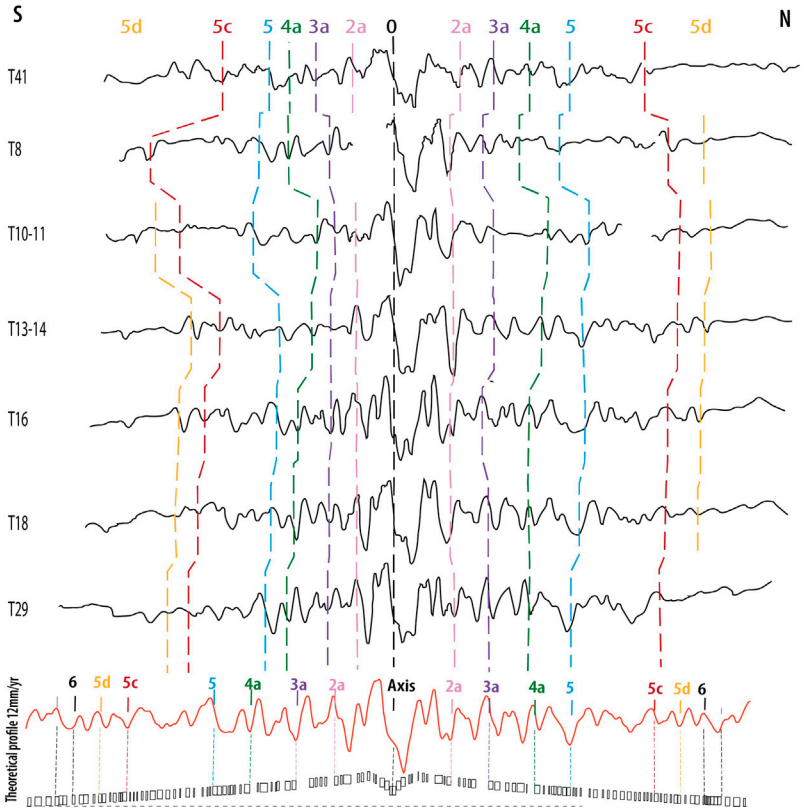

FIGURE 4 | Magnetic anomaly profiles corresponding to seismic transects shown in **Figure 2**. Anomaly identifications are based on the synthetic model shown in red below the profiles. The model was calculated with a symmetrical half rate of 12 mm/yr, which emphasizes the asymmetry of spreading along the segment: spreading on the southern flank has been significantly slower than on the northern flank.

We interpreted the top basement reflector on each seismic line to produce a map of top basement depth (**Figure 3A**) and a map of sediments thickness. Two-ways travel time (TWTT) in seconds were converted to meters, using the sediment velocity model described in Japsen (1993). The sediment thickness (in meters) is thus calculated following the equation:

$$y = 0,0227x^3 + 0,0378x^2 + 0,9982x - 0,0469$$

where x represents the sediment thickness in time observed on the seismic lines.

Gravimetric measurements were not performed during the MAD survey. To construct the gravity maps and associated derivatives maps we used a satellite-derived free-air anomaly (FAA) gravity grid (Sandwell and Smith, 2009), and the Bureau Gravimétrique International (BGI) Bouguer anomaly grid (**Figure 3B**, available online on the website https://bgi.obs-mip.fr/) which is computed from the satellite-derived free-air gravity using the GEBCO bathymetry (available online on the website https://www.gebco.net/). The first horizontal derivative of the FAA (**Figure 3C**) is the square root of the sum of the squares of the derivatives in the x, y. The analytic signal (Klingele et al., 1991; Marson and Klingele, 1993) of the BGI Bouguer anomaly (**Figure 3D**) is the square root of the sum of the squares of the derivatives in the x, y, and z directions. Local peaks are interpreted as edges of source bodies and therefore allow us to define the anomaly sources (Beiki, 2010).

To better constrain the oceanic domain, the FAA has been corrected from the density variation associated with cooling of the lithosphere with age. For this we first calculated an age grid using the magnetic anomaly identifications. We then calculated a grid to account for the effect of upper mantle cooling with age, assuming a simple square root of age mantle cooling law (Parsons and Sclater, 1977), a mantle thermal expansion coefficient of $3.1e^{-5}$/°C and a mantle density of 3,300 kg/m^3 and applied that to the gridded gravity data. In order not to over correct our gravity data for near ridge upper mantle temperatures, we cut our thermal model 10 km off-axis, and used a constant temperature gradient in the intervening axial region. The calculated thermal gravity anomaly is removed from the FAA to obtain a corrected Bouguer anomaly that is used to perform gravity modelling. We used the GM-SYS modelling software (Geosoft Oasis Montaj®) to model the depth to the base of crust from the gravity anomaly measured along each seismic transects. We used the observed geometry for seafloor and top basement interfaces and the following density values: 1,030 kg/m^3

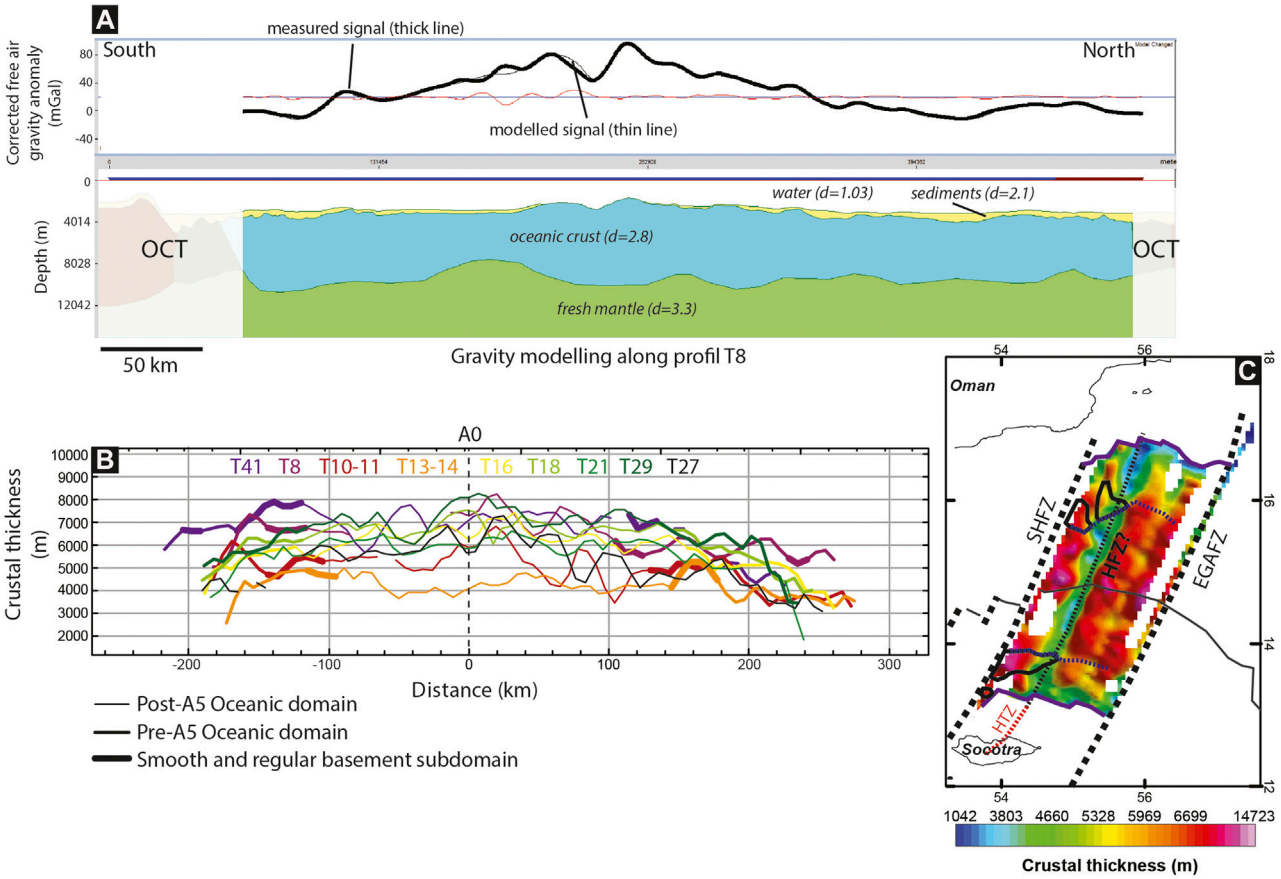

FIGURE 5 | (A) Example of gravity modelling along transect T8. Thick black line represents the measured gravity signal, thin black line represents the modelled gravity signal. The error near the ridge axis is certainly linked to the data gap in the seismic acquisition in this area. **(B)** Compilation of the different profiles of crustal thickness computed for the seismic transects. **(C)** Computed crustal thickness map. HFZ, Hadibo Fracture Zone.

for water, 2,100 kg/m^3 for sediments, 2,800 kg/m^3 for the oceanic crust and 3,300 kg/m^3 for the mantle (**Figure 5**).

SEISMIC OBSERVATIONS: CHARACTERISTICS OF THE OCEANIC CRUST AND MORPHOLOGICAL VARIATIONS IN SPACE AND TIME

The Pre-A5 Oceanic Domain

Nonn et al. (2017) noticed that the first oceanic crust is sometimes marked by the presence of a basement ridge which can overlap the OCT crustal units and/or syn-rift sedimentary units in the adjacent exhumed domain (**Figure 2**, black arrows in profiles T10–11, T18 and T29). Because this ridge is symmetrical with reflective flanks and no internal structure, it has been interpreted as a volcanic seamount (Nonn et al., 2017).

The distribution of the magnetic anomalies (**Figures 1B**, **2**, **4**, **6**) in the adjacent oceanic domain of the Socotra-Sharbithat segment highlights a clear asymmetry. The oceanic domain is wider on the north flank of the ridge than on the south flank. This is particularly visible for the western transects T8 and T10-11 (**Figure 2**). Moreover, most of this asymmetry appears to have been acquired before magnetic anomaly A5 (10.95 Ma) (**Figures 2**, **4**, **6**). This anomaly also coincides with major changes in the basement characteristics and can be interpreted as an approximate boundary between an old oceanic domain (pre-A5) and a young oceanic domain (post-A5).

The oceanic crust in the old oceanic domain (pre-A5) is mainly characterized by chaotic and commonly hard to interpret top basement reflections (**Figure 7A**), with a sediments/top basement interface which is unclear. The top basement is generally imaged by small discontinuous reflections of high amplitude. Its roughness is caused by small cone-shape or rounded seamounts and by numerous normal faults that create fault scarps (**Figures 7A, B**). These normal faults generally have throws less than 0.3 s TWTT (~280 m), irregular distribution and varying block size. They alternate with seamounts or are sometimes partly covered by them. With the exception of few areas where the fault planes are particularly reflective (**Figure 7C**), the root of the normal faults along the MAD profiles are not visible due to the low seismic penetration. The deep penetration along the ENCENS lines, however, allows

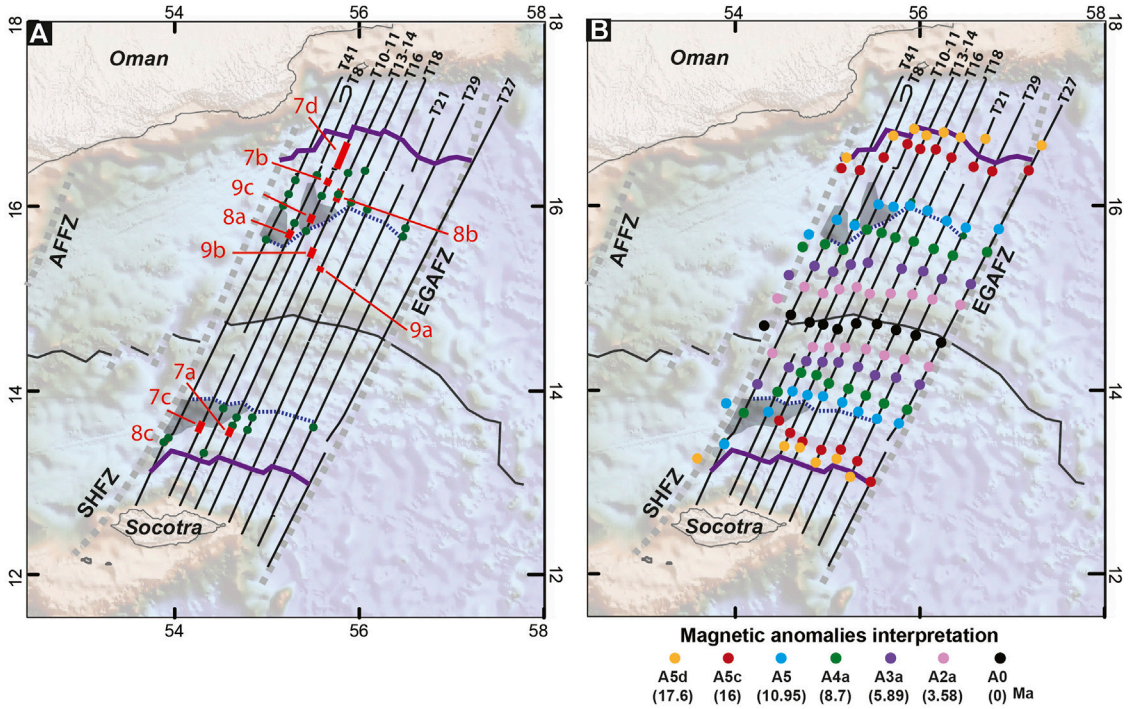

FIGURE 6 | (A) Map showing the location of the zooms displayed in **Figures 7**,**8**,**9**. Green points show the location of the sedimentary deformation. **(B)** Map showing the correlation between the magnetic anomalies and the structural boundaries defined by seismic observations. Violet line represents the location of the first oceanic crust identified on the seismic profiles [note that the OCT location of Nonn et al. (2017) followed exactly the A5d magnetic anomaly identification for the T21, T29 and T27 transects]. Dashed blue line represents the boundary between the old and young oceanic domains determined by seismic observations. Gray areas highlight the smooth and regular basement subdomain. Ages of the oceanic magnetic anomalies are from Cande and Kent (1995).

us to observe the entire structure of this basement (**Figure 7D**): It is characterized by an upper transparent layer (approximately 1 s TWTT or 3 km thick) marked at its base by a high amplitude, discontinuous reflector. The lower layer is more reflective and its base is sometimes marked by highly discontinuous reflections at 2 s TWTT (6 km) below top basement. Along the ENCENS lines some fault planes are visible and appear to root on the reflective interface at 1 s TWTT (3 km) below top basement (btb) (**Figure 7D**). The detailed MAD lines show that the oceanic basement in this domain is marked by the presence of disorganized and distributed numerous small reflections/hyperbolas (black arrays in **Figure 7A**).

The sedimentary architecture expected in oceanic domains is passive infill, with flat lying, parallel stratification onlapping against basement highs or current-related structures such as contourites (Rebesco et al., 2014). Deformation of this sedimentary infill is expected to occur at the ridge axis and therefore not to affect the sediments deposited off-axis. This kind of sedimentary structure is observed in the oldest part of the pre-A5 domain (**Figures 7A, D**). However, the sedimentary sequence overlying the oceanic crust in the Socotra-Sharbithat segment displays substantial deformation. This deformation is clearly post-spreading and as shown in **Figure 7B** may have occurred in a relatively late stage. It may be related to tectonic processes such as faulting, as shown by the syn-tectonic wedges observed in **Figure 7B**. However, the most common sedimentary deformations in the pre-A5 oceanic domain are columns of perturbed sediments, locally present above basement seamounts or normal faults (**Figure 7C**). These structures are generally associated with fluid-escapes. Note that these columns of deformed sediments often end in large-scale horizontal lenses of highly perturbed sediments where the stratification is no longer observable (**Figure 7C**). In this domain, we also observe numerous large-scale unconformities, or unconformities restricted to smaller areas above basement seamounts (**Figures 7C**, **8A**, **B**), suggesting late phases of vertical movements of the basement (uplift or subsidence). In several places the sediments at the interface with the basement are also perturbed by the presence of high amplitude small, spoon-shaped reflections that make it difficult to identify the top-basement horizon in this domain (**Figure 8C**).

A kind of subdomain displaying particular characteristics can be delimited in the pre-A5 oceanic domain (areas outlined in black in **Figure 3** and shaded grey areas in **Figure 6**), to the western part of the Socotra-Sharbithat segment. The youngest portions of the pre-A5 oceanic domain are indeed characterized by more reflective, smooth and regular top basement, with no fault scarps, and occasional rounded seamounts (**Figure 9C**). The top basement reflection is created by a series of superimposed flat lying reflectors sometimes creating stair-step shapes (**Figure 9C**).

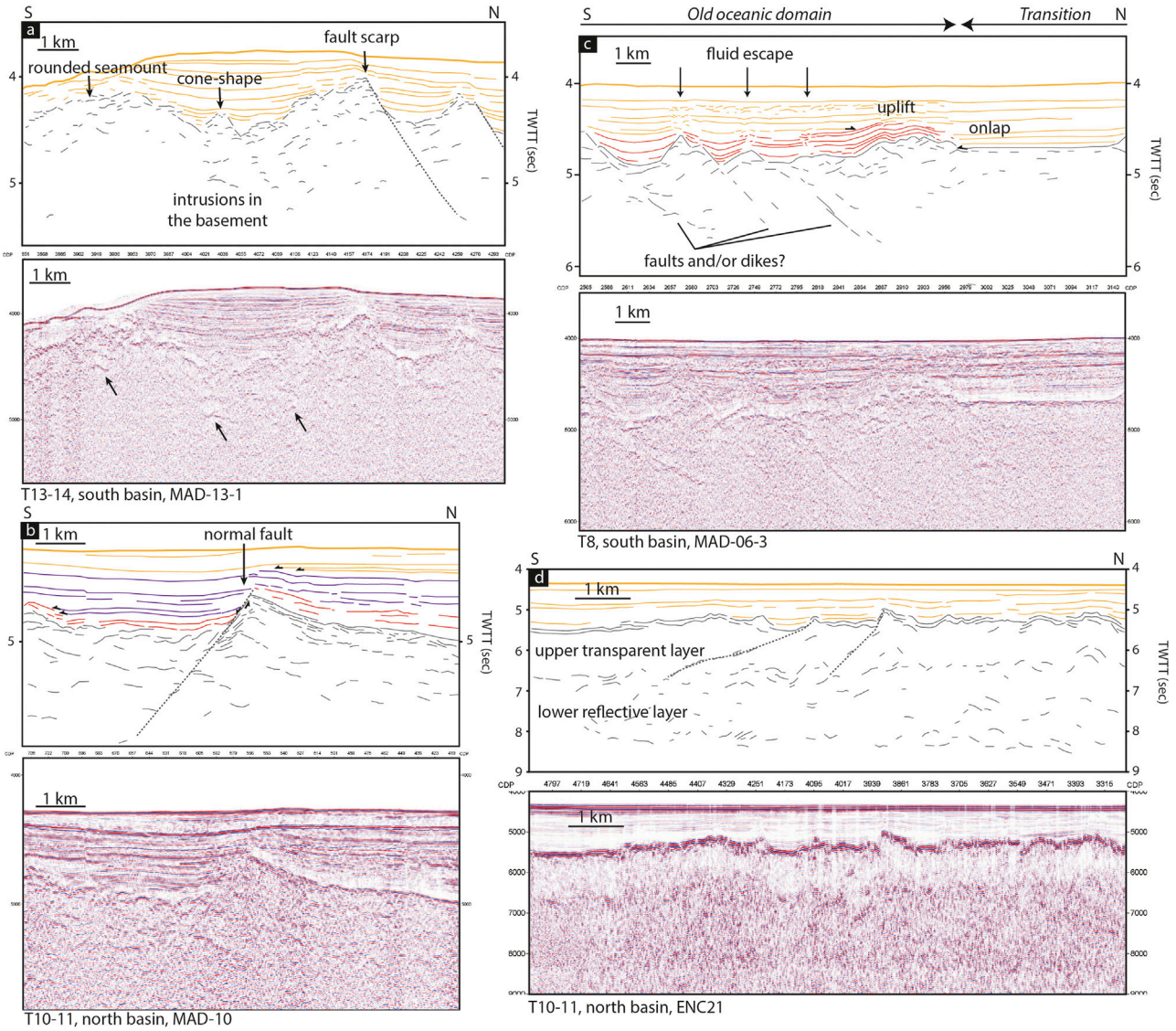

FIGURE 7 | Example of top basement morphology in the old oceanic domain. **(A)** Close up along the seismic transect T13–14, south basin. **(B)** Close up along the seismic transect T10–11, north basin. Orange sediments represent undeformed sedimentary unit onlaping on oldest (red and violet) units showing syn- or post-deposition deformation. **(C)** Details of the contact between the old oceanic domain and the smooth and regular basement subdomain along the transect T8, south basin. Note the difference in top basement morphology and the onlap of the smooth and regular basement subdomain onto the old oceanic crust. This figure shows deformation in sediments (in red) and the presence of deformed sediments in columns ending on large-scale horizontal lenses of highly perturbed sediments. **(D)** Details of the old oceanic crust along an ENCENS seismic line. The figure shows the upper transparent layer of 1 s (twtt) thick and the lower more reflective layer. Location of the close-up views is shown in **Figure 6**.

The internal hyperbolas observed in the oceanic crust of the older and adjacent pre-A5 domain are not observed in these smooth and regular top basement subdomains (**Figure 9C**). The transition from older pre-A5 basement to this smooth and regular top basement subdomain is generally sharp, the smooth basement onlapping and possibly overlapping the older oceanic basement (**Figure 7C**). The dominant sedimentary structure over the smooth and regular basement is passive infill (**Figure 9C**), with little to no evidence for faulting. However, the sedimentary deformation in the pre-A5 oceanic domain is mainly restricted to areas 20–25 km away from this smooth and regular top basement subdomain (**Figures 7C**, **6**).

Post-A5 Oceanic Domain

The younger oceanic crust (post-A5 anomaly, **Figure 6**) is characterized by a homogeneous and regular top basement which is highly reflective and easy to interpret thanks to a

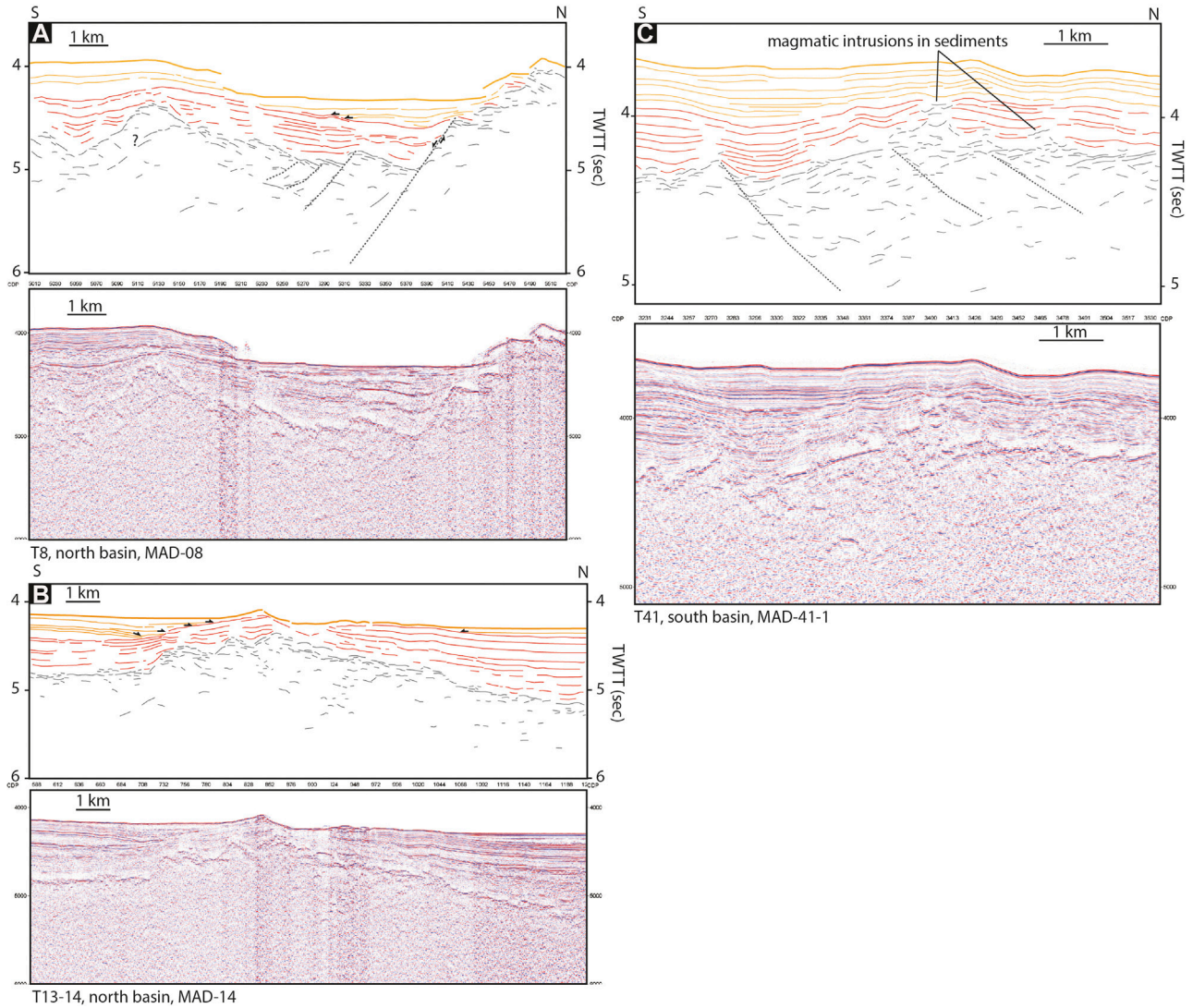

FIGURE 8 | (A) and **(B)** Examples of sedimentary unconformities in the old oceanic domain suggesting vertical (uplift) movements of the basement after or during the deposition of the red unit. **(C)** Example of intrusions into the sediments in the old oceanic domain. The top basement/sediments interface is not clear in such areas. Location of the close-up views is shown in **Figure 6**.

well-defined sediments/top basement interface (**Figure 9B**). The smooth, planar and reflective areas of top basement is interrupted regularly by fault scarps (**Figure 9B**). These normal faults generally have throws around 0.4 s TWTT (400 m), but some are larger (until 0.7 s TWTT, 700 m). The faulted blocks are well defined, except when they are sealed by rounded or cone-shape seamounts (**Figure 9B**). These seamounts generally seal the fault breakaways (i.e. the point where a fault breaks the syntectonic surface) (**Figure 9B**). The MAD lines do not image the entire internal structure of the oceanic crust and there is no ENCENS seismic lines in the post-A5 oceanic domain. However, in contrast to the pre-A5 oceanic domain, the oceanic crust in the post-A5 domain seems more homogeneous, with only a few small, scattered hyperbolas present in the basement.

As typically expected for sedimentary sequences that rest on oceanic crust, passive infill is observed in this post-A5 oceanic domain (**Figure 9B**). Occasionally, some very thin syn-tectonic sedimentary wedges can be observed at the top of faulted blocks. Current-related sedimentary structures are notably present in this domain (**Figure 9A**).

DOMAIN MAPPING: POTENTIAL FIELD DATA AND CRUSTAL THICKNESS

The profiles of crustal thickness and the associated map (**Figure 5**) show that the old, pre-A5 oceanic domain is marked by variable crustal thicknesses, from 4 to 7 km, and as

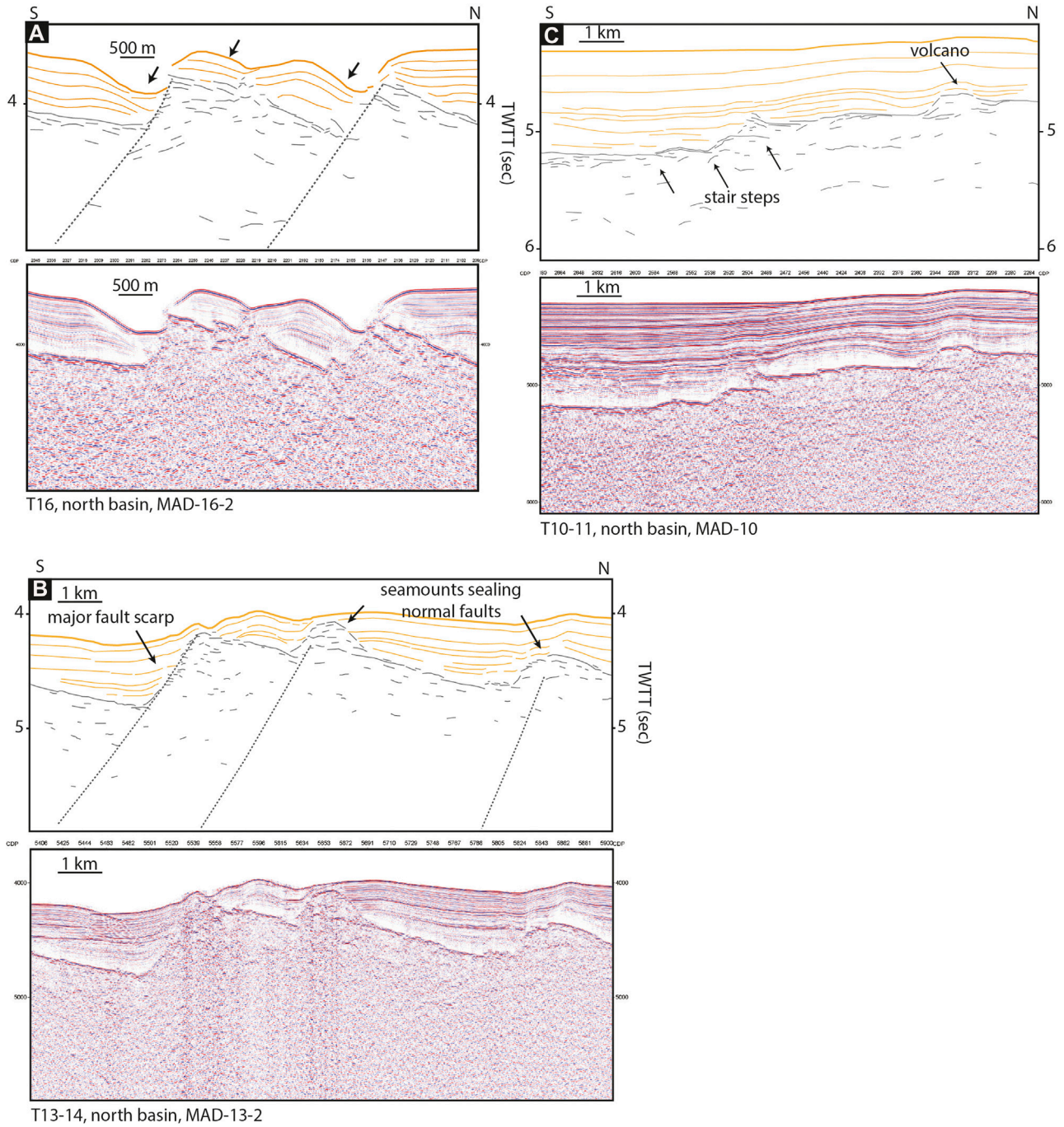

FIGURE 9 | (A) Example of currents-related sedimentary architectures associated with normal faults affecting the basement in the young oceanic domain. **(B)** Example of top basement morphology in the young oceanic domain. Note the presence of rounded seamounts sealing several fault breakaways. **(C)** Details of the top basement morphology in the smooth and regular basement subdomain, along the transect T10–11, north basin. Stair steps buildings and presence of a rounded seamount. Location of the close-up views is shown in **Figure 6**.

much as 8 km in the smooth and regular basement subdomain. The young, post-A5 oceanic domain is generally marked by a 6–7 km thick crust, excepted in the area of transects T10–11 and T13-14 where the crust is about 4–5 km thick. This area of thin oceanic crust has the same NE-SW orientation as the main Socotra-Hadbeen and Eastern Gulf of Aden fracture zones

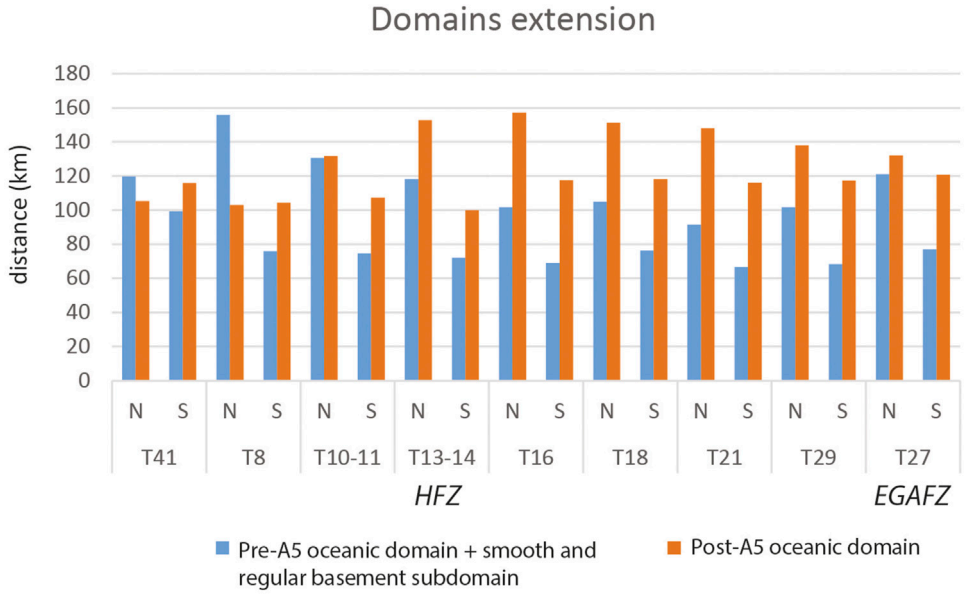

FIGURE 10 | This figure represents and compares the widths (in km) of the two main domains observed in the oceanic domain for each seismic transect: pre-A5 (+ smooth and regular basement subdomain) and post-A5 oceanic domains. For each seismic transect, the width of each domain on the north and south flanks is compared to observe the symmetry or asymmetry. Note the strong asymmetry of the post-A5 domain close to the interpreted HFZ. The pre-A5 domain shows also a short asymmetry, with the south flanks shorter than the north flanks.

(**Figure 5C**). It marks the eastward termination of the over-thickened (>7 km-thick) crust in the smooth and regular basement subdomain. It also correlates with the transition from a rather symmetric young oceanic domain to the west, to a quite asymmetric domain to the east (**Figure 10**). This NE-SW trend associated with the thin oceanic crust is also observed on the horizontal derivative of the FAA (thin dashed line on **Figure 3C**). This map also reveals linear, E-W trending anomalies, especially in the post-A5 oceanic domain (north and south flanks), east of this lineation. These E-W anomalies correlate with major seamounts on seismic lines, highlighting their lateral continuity. It is interesting to note that the boundary between pre-A5 and post-A5 domains is associated with such lineation of basement highs (**Figures 3C**, **2**). The transition between the OCT domain and the pre-A5 oceanic domain to the south is marked by a clear, continuous gravity anomaly. This is in agreement with the observation of a basement ridge marking this transition (**Figure 2**).

On the Bouguer gravity anomaly map (**Figure 3B**), the pre-A5 domain is associated with higher gravity values than the younger, post-A5 oceanic domain (**Figure 3B**). We note a global change from west to east, with low gravity values in the adjacent Encens-Sheba segment and high values east of the EGAFZ (**Figure 3B**). The analytic signal map (**Figure 3D**), calculated from the Bouguer anomaly map, shows several patches of high values, especially in the vicinity of fracture zones (EGAFZ to the east and SHFZ to the west) (black arrows; **Figure 3D**).

Figure 6B highlights clear magnetic isochrons in the young, post-A5 oceanic domain. In contrast, the isochron of the magnetic anomalies are discontinuous in the smooth and regular basement subdomain, located in the western part of the segment (**Figure 6B**). The interpreted magnetic anomalies highlight an asymmetry in the spreading rates, which is in agreement with the asymmetric width of the oceanic domains (**Figures 2**, **4**). We observe that the total area of the pre-A5 oceanic domain and the smooth and regular basement subdomain on the south flank is always less than the total area of the pre-A5 oceanic domain and the smooth and regular basement subdomain on the north flank (**Figure 10**). For the post-A5 oceanic domain, the width is quite similar for the western transects (for T41 and T8). Towards the east, the north domain becomes larger than the south domain, with a strong asymmetry close to the NE-SW lineation observed in the gravity data (around transect T13-14).

INTERPRETATION AND DISCUSSION

Nature of the Oceanic Basement and the Formation of the Oceanic Crust

The compilation of our observations shows that there are two main distinguishable oceanic domains within the Socotra-Sharbithat segment. The old, pre-A5 domain is characterized by a complex and heterogeneous basement. The top basement is chaotic and often affected by normal faults and rounded seamounts that are interpreted as volcanoes. The crustal thickness varies from anomalously thin (4 km) to normal (7 km) (**Figure 5**) suggesting low to normal magmatic budget. It is associated with slow spreading rates (between 10 and 15 mm/year, half-rate). The younger, post-A5 oceanic domain is quite different. It is relatively uniform, with a reflective top basement

affected regularly by sets of normal faults (**Figure 9B**). Magmatic extrusions appear frequent in this domain, but tend to be restricted to faulted areas, suggesting that the emplacement of magmatic material occurs especially along normal faults. The thickness of the crust in the post-A5 domain is normal (6–7 km) (**Figure 5**) and associated with slow spreading rates, mostly between 10 and 15 mm/year (half-rate).

Despite structural variations, the whole oceanic domain in the Socotra-Sharbithat segment appears to have been formed under slow-spreading conditions. With a full spreading rate of 25 mm/year, the Mid-Atlantic Ridge (MAR) shows spreading conditions similar to the ones observed in the Socotra-Sharbithat segment, where three different tectonic styles have been identified in the south of the Kane Fracture Zone (Cann et al., 2015):

- Volcanic mode of spreading characterized by volcanic constructions forming parallel elongate abyssal hill ridges, coupled with minor faulting. The faulted blocks show very limited seafloor rotation;
- Detachment faulting marked by tectonic extension along simple long-lived faults, leading to the formation of core complexes with unroofing of gabbros and ultramafic rocks (Cannat et al., 1995; MacLeod et al., 2002; Dick et al., 2008);
- Extended terrain with abundant large-offset faults forming narrow ridges associated with oval basins. The crustal thickness in these areas appear more variable. This style would be intermediate between detachment faulting and volcanic construction.

Comparison with our observations in the Socotra-Sharbithat segment suggests that the pre-A5 oceanic domain could be similar to the extended terrain described by Cann et al. (2015), with potentially the presence of detachment faults creating more rotated blocks. Moreover, Sleep and Barth (1997) showed that at such spreading rates it is not possible to sustain a steady state magma chamber at the ridge axis and that the resulting oceanic crust can be composed by a mix of mafic and ultramafic rocks (up to 20% ultramafic material for the young Atlantic crust). Slow-spreading oceanic crust are generally characterized by less distinct Moho and with more variability in both its structure and reflectivity (Mutter and Karson, 1992; Morris et al., 1993; Combier et al., 2015). It suggests that mafic and ultramafic rocks can occur in such environments (Cannat, 1993). This is consistent with our observations of irregular and discontinuous Moho reflections at 2 s TWTT (6 km) (**Figure 7D**) and with crustal thickness variations in the pre-A5 oceanic domain. The overall reflectivity of the lower crust is also much higher than at faster spreading oceanic crust. It is inferred to be due to tectonic features and greater compositional heterogeneity compared to crust formed at higher spreading rates (Mutter and Karson, 1992). As observed in the presented seismic profiles, the upper part of the crust is also characterized by the presence of sub-horizontal reflectors lying 1.5–2 km below the top of the oceanic basement and by dipping reflectors of high-amplitude extending from the top basement into the mid-crust (**Figure 7D**) (Morris et al., 1993; Momoh et al., 2017, 2020). Our pre-A5 oceanic domain could thus be similarly associated with a hybrid crust (i.e., a mix of mafic and ultramafic rocks) thought to occur at slow-spreading rates such as those calculated here. While the mafic component can be quite clearly deduced from seismic observations (volcanic seamounts and constructions, numerous hyperbolas in the basement and in the sediments, reflective top basement), the presence of ultra-mafic rocks cannot be confirmed due to the lack of dredge sampling and drilling. Nevertheless, we note that the basement in the pre-A5 oceanic domain is clearly deeper than the one in the post-A5 oceanic domain and that the Bouguer anomaly is higher (**Figures 3A, B**), suggesting a variation of composition and/or spreading processes between the two domains, perhaps a higher percentage of ultra-mafic materials in the old domain.

Alternatively, the post-A5 oceanic domain could correspond to a slow spreading volcanic mode. The post-A5 oceanic basement is indeed regularly affected by slightly rotated normal faults. Thatcher and Hill (1995) suggested that the faulted morphology of such slow-spreading basement illustrates alternating phases of tectonism and magmatism. However, more recent studies demonstrate that normal faults in oceanic domains are not necessarily associated with pure amagmatic episodes and that they can develop under variable magmatic conditions at the axis (e.g., Buck et al., 2005; Behn and Ito, 2008; Cannat et al., 2019). The fact that volcanic constructions occur above the faulted blocks and that at these locations the top basement is less well defined, with strong reflections in the sediments, suggest that there is a strong magma-fault relationship, magmatism being active during the development of these faults, the magma being channeled at the top of the basement through the normal faults. The absence of deformation in the sediments in the post-A5 oceanic domain shows that tectonic activity does not affect older basement and remains localized at the axis. These observations are consistent with the results of Singh et al. (2006) at the Lucky Strike slow-spreading segment (MAR), where interactions between tectonic processes (faulting) and magmatism (presence of a magma chamber) have been observed in the axial valley.

The Smooth and Regular Basement Subdomain, Marker of a Magmatic Pulse at 11 Ma?

In comparison to pre- and post-A5 oceanic domains, patches of smooth and regular basement display an over-thickened crust (8 km) (**Figure 5**), associated with a reflective top basement showing stair-steps architectures (**Figure 9A**). In contrast to the adjacent oceanic domains, this subdomain is devoid of normal faults, suggesting that it formed by a purely magmatic process. The stair-steps architecture shows that the crust is formed by superimposed lava flows. These observations suggest that the smooth and regular basement subdomain represents a magmatic plateau which has been subsequently rifted by the ridge axis, similar to the interpretation proposed by Cannat et al. (1999) for the Azores Platform in the Lucky Strike segment on the MAR. Laterally, this structure coincides with the transition between pre- and post-A5 oceanic domains, which is marked by an E-W lineation of basement highs, likely volcanic in origin. These observations suggest that the oceanic crust in the smooth and regular basement subdomain and the onset of

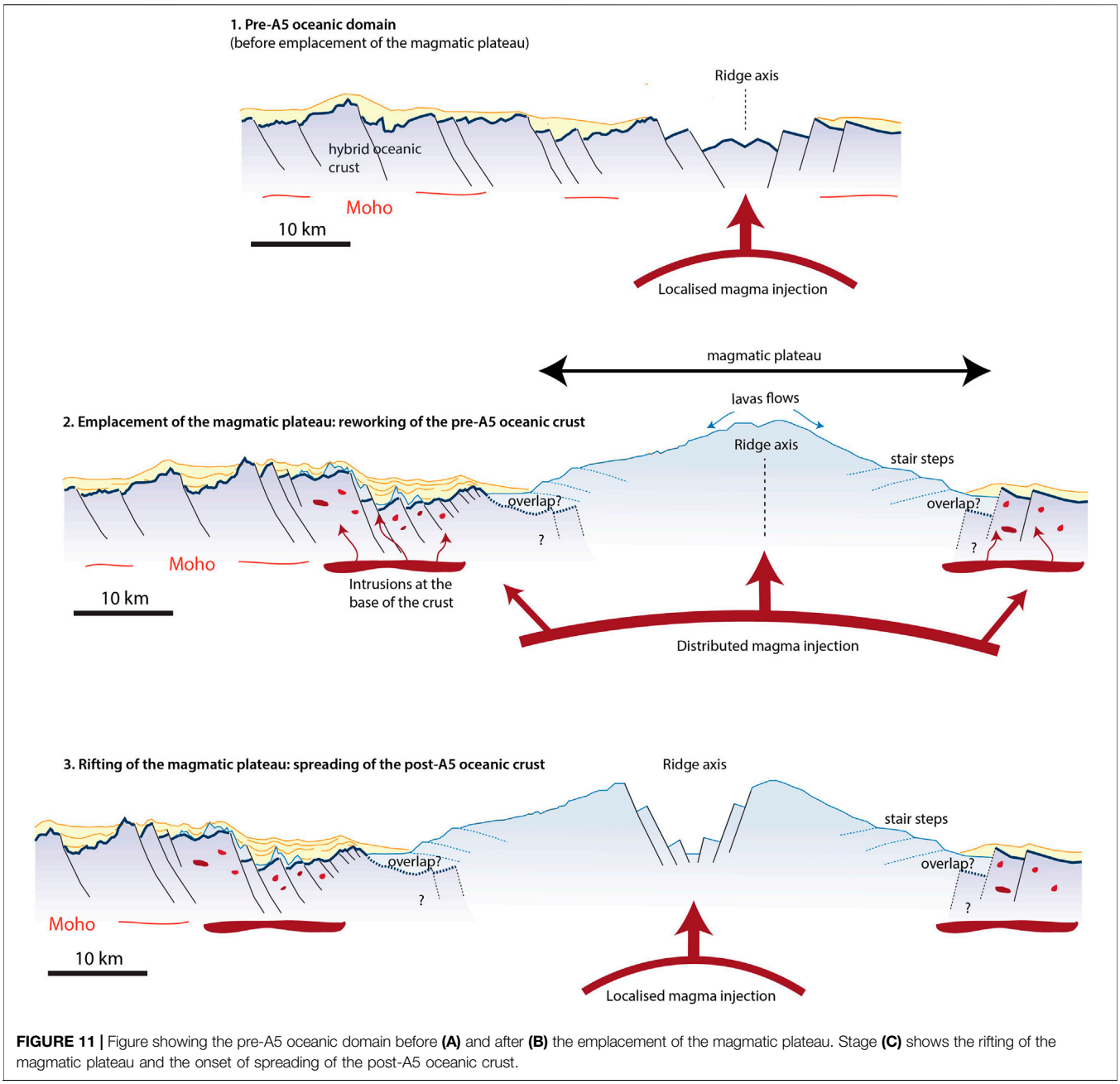

FIGURE 11 | Figure showing the pre-A5 oceanic domain before **(A)** and after **(B)** the emplacement of the magmatic plateau. Stage **(C)** shows the rifting of the magmatic plateau and the onset of spreading of the post-A5 oceanic crust.

spreading in the post-A5 oceanic domain have been formed during a period of intense magmatism, probably associated with an excess of magma at the ridge axis (or magmatic pulse). This event seems to have occurred around 10.95 Ma (anomaly A5).

This magmatic pulse seems to have occurred all along the axis but the presence of the smooth and regular basement subdomain suggests that the magmatic budget was significantly higher in the western extremity of the segment. Moreover, the overlap architecture visible at the transition from the pre-A5 oceanic domain to the smooth and regular basement subdomain (**Figure 7C**) suggests that the lavas erupted during this episode of intense magmatism could have flowed over the previously formed oceanic basement. Garmany (1989) shows that subsurface magma can be transported several tens of kilometers away from the axis, depending on the melt viscosity and Moho topography (Spence and Turcotte, 1985), potentially leading to the formation of off-axis volcanoes. Based on the seismic profiles presented here, we suggest that the magmatic intrusions and extrusions may extend 40 km or more off-axis (**Figure 11**). Although the available data do not permit us to determine the extent of this overlap, such extensive

magmatic activity could also partly explain the over-thickened oceanic crust in the smooth and regular basement subdomain.

The old, pre-A5 oceanic domain is also marked by a clear post-rifting spreading deformation, especially in the vicinity of the smooth and regular basement subdomain and post-A5 oceanic domain. The observed deformation is related to fault displacements (**Figure 7C**) but also mainly to vertical movements (generally local uplifts, e.g., **Figures 8A, B**). Close to the smooth and regular basement subdomain, we also noticed the presence of numerous hyperbolas, distributed in the basement (**Figure 7A**) and at the interface between sediments and top basement (**Figure 8C**). These small hyperbolas can be interpreted as magmatic intrusions/sills. At some locations (e.g., **Figure 7C**) the normal faults appear particularly reflective and the sedimentary columns above the fault scarps are perturbed by fluid escape. This also suggests the presence of magmatic intrusions, using pre-existing normal faults as feeder systems. This kind of structure and deformation ends abruptly in the smooth and regular basement subdomain and in the post-A5 oceanic domain. The observation of such deformation in steady state oceanic domains is surprising, as all the deformation in these domains should be localized at the ridge axis. The presence of deformed sediments in the pre-A5 oceanic domain can be interpreted by several hypotheses: 1) the axis was sedimented during the formation of the crust; 2) the deformation is associated with the presence of fracture zones; 3) a younger, large magmatic event led to intrusions and "cracking" of the old crust in the vicinity of the contact. Our preferred hypothesis is the last one, the lavas associated with the 11 Ma magmatic pulse being sufficiently fluid and with such an overpressure, melt could have been driven far away from the ridge axis, affecting the basement in the pre-A5 oceanic domain and leading to deformation of the primary oceanic crust (**Figure 11**). This may be the origin of the deformation visible in the sediments and the magmatism observed in this domain (intrusions into the basement, in the sediments and at the base of the crust), leading to the current morphology of the pre-A5 oceanic basement. The primary morphology of the oceanic crust in this domain is thus now difficult to identify, as it has been reworked by the magmatic event.

Interestingly, the age of this supposed magmatic pulse in the Socotra-Sharbithat segment (anomaly A5, 10.95 Ma) and the initiation of the post-A5 oceanic domain coincides with the large off-axis magmatic event proposed in the Sheba segment west of the SHFZ. This event is dated between 10 and 5 Ma (A5 to A3) (d' Acremont et al., 2010; Leroy et al., 2010b). It is well marked in the bathymetry and supposed to have induced a small ridge jump of the Sheba segment to the south around A5 time that may explain the asymmetry of the observed domains in the Sheba segment. Although some asymmetry has been observed in the Socotra-Sharbithat segment it is not clear if it can be related to a ridge jump similar to the one proposed for the adjacent western Sheba segment.

Mantle Plume Effects on Rift and Ridge Processes

The smooth and regular basement subdomain, which is considered as a magmatic plateau, is bound to the east by a NE-SW elongated zone of thin oceanic crust (**Figure 5**). Result of this and previous studies (Leroy et al., 2012; Bellahsen et al., 2013; Pik et al., 2013; Ahmed et al., 2014) suggest that this elongated area could correspond to the location of a fracture zone, the Hadibo Fracture Zone (HFZ), which has been observed at the Oman and Socotra margins and on land. It correlates with a low in the horizontal gradient of the gravity (**Figure 4C**). This proposed fracture zone also marks the boundary between post-A5 symmetric spreading to the west and post-A5 asymmetric spreading to the east (**Figure 10**). Spreading asymmetry such as that seen in the post-A5 oceanic domain east of the HFZ could have been associated with oceanic lithosphere preferentially forming one flank by the mechanism of a detachment fault to create an oceanic core complex (OCC). Cann et al. (2015) attribute highly asymmetric spreading south of the Kane Fracture Zone on the Mid-Atlantic Ridge to the formation of major core complexes at the inside corner of ridge-transform intersections where magmatism is expected to be weak because of older, cooler lithosphere on the other side of the transform (e.g., Tucholke et al., 1998; Blackman et al., 2002). The near-axis gravity high on the northern flank next to the HFZ (arrow 1, **Figure 3**) might be interpreted as an OCC, to which the observed asymmetry could be ascribed. However, this feature appears to be at the outside corner of the segment, which is unusual for OCC formation. Moreover, a significant amount of offset on the transform fault is necessary to develop an OCC (Cormier and Sloan, 2019) and the HFZ seems to have a very small offset. Thus, OCC formation seems an unlikely explanation for the post-A5 spreading asymmetry here.

It has been proposed that the off-axis magmatic event in the Encens-Sheba segment could be related to the Afar plume activity (Leroy et al., 2010b). Although the Afar plume is located more than 1,000 km to the west, melt could have been channeled as far along the ridge axis as the AAFZ (Leroy et al., 2010b). The main signature of the magmatic pulse in the Socotra-Sharbithat segment is restricted to the segment between the SHFZ (Socotra-Hadbeen Fracture Zone) and the newly identified HFZ, in the western part of the Socotra-Sharbithat segment. It is thus possible that the magmatic pulse observed here represents the eastward termination of the major off-axis magmatic event in the adjacent segment, the melt being channeled through the SHFZ. A similar process has been suggested for the rifted volcanic plateau in the Lucky Strike segment (Mid-Atlantic) (Cannat et al., 1999). It would have formed during an event of anomalously high melt production, quite likely due to a change in the temperature, composition or dynamics of the mantle supplied to the Mid-Atlantic Ridge by the Azores hotspot. This episode of enhanced magmatism seems to have migrated along the ridge axis.

This magmatic event marks the transition between the pre-A5 and post-A5 oceanic domains in the Socotra-Sharbithat segment. If the transition between the two domains appears to have occurred around the A5 anomaly (10.95 Ma) east of the HFZ, it does not appear to be a synchronous event all along the Socotra-Sharbithat segment. Indeed, west of the HFZ, the magmatic pulse could have started at A5c (16 Ma) and lasted until A4a (8.7 Ma). Although there is no clear change in the spreading rate, there seems to have a slight modification in the spreading processes between the two oceanic domains. It is thus possible that the major large-scale magmatic event at ~11 Ma, potentially related to the Afar plume,

perturbed the magmatic system and led to a modification of the spreading mode for the whole Socotra-Sharbithat segment. Another idea to explore could be the influence of the continental margin proximity on the magmatic budget at the spreading ridge. Would a young spreading center be less magmatic than at a more mature stage due to the close location of the margin? What is the effect of the proximity of a cold continental lithosphere for melt production below a young oceanic ridge? All these questions deserve to be in-depth investigated in new studies.

CONCLUSION

The observation and interpretation of margin-to-margin seismic transects and the correlation with potential field data sets and gravity modelling allowed reconstruction of the 16 Ma-long spreading history of the Socortra-Sharbithat segment in the eastern Gulf of Aden oceanic basin. The first noticeable event is the onset of steady state seafloor spreading, which is marked by a small magmatic pulse leading to the formation of a volcanic ridge at the end of the oceanic-continental transition. We identify an old oceanic domain (pre-A5) which could have been formed during a phase of low magmatic budget and could represent a hybrid oceanic crust with a significant component of ultramafic material. The younger oceanic domain (post-A5) appears to have formed during a more volcanic phase, at the same slow spreading rate. The transition between the two spreading modes occurred around 11 Ma and is associated with a magmatic pulse, which led to the formation of a magmatic plateau in the western extremity of the segment. This magmatic event could be related to the major off-axis event previously identified in the adjacent Encens-Sheba segment, and possibly related to the Afar plume. This event seems to have partly reworked the oceanic crust previously formed in the pre-A5 oceanic domain through magmatic intrusions and extrusions.

DATA AVAILABILITY STATEMENT

The data supporting the conclusions of this article will be made available by the authors, without undue reservation.

AUTHOR CONTRIBUTIONS

MG: Seismic interpretation, Visualization, Gravity modelling, Writing. SL: Seismic processing, Magnetic processing and interpretation, Writing, MC: Gravity modelling, Writing. HS: Magnetic processing and interpretation.

FUNDING

This research was funded by ANR Rift2Ridge (NT09-4854), and ANR YOCMAL-07-BLAN-0135. MG was funded by an ISTeP grant.

ACKNOWLEDGMENTS

We would like to kindly acknowledge Julie Tugend, Daniel Sauter and Philippe Patriat for discussions concerning the topics of this paper. We also thank the BGI for the Bouguer anomaly grid. We are indebted to the Flotte Océanographique Française, and to the officers, and the crew members of the BHO Beautemps-Beaupré, and to the French Navy hydrographers and the hydrographic team of the Mission Océanographique de l'Atlantique for their assistance in data acquisition in 2012 during Marges-Aden cruise. We deeply thank the Yemeni colleagues Khaled Khanbari, I. Al Ganad and the authorities for authorisations of work. We deeply thank the Omani colleagues, Issa El Hussein, Ali Al-Lazki, Samir Sobhi, A. Al Rajhi, Hilal Al-Azri, M. Al-Araimi and K. Al Toubi and the authorities for authorisations of work. MG was funded by Sorbonne Universite and ISTeP.

REFERENCES

Ahmed, A., Leroy, S., Keir, D., Korostelev, F., Khanbari, K., Rolandone, F., et al. (2014). Crustal Structure of the Gulf of Aden Southern Margin: Evidence from Receiver Functions on Socotra Island (Yemen). *Tectonophysics* 637, 251–267. doi:10.1016/j.tecto.2014.10.014

Autin, J., Leroy, S., Beslier, M.-O., d'Acremont, E., Razin, P., Ribodetti, A., et al. (2010). Continental Break-Up History of a Deep Magma-Poor Margin Based on Seismic Reflection Data (Northeastern Gulf of Aden Margin, Offshore Oman). *Geophys. J. Int.* 180, 501–519. doi:10.1111/j.1365-246x.2009.04424.x

Behn, M. D., and Ito, G. (2008). Magmatic and Tectonic Extension at Mid-ocean Ridges: 1. Controls on Fault Characteristics. *Geochem. Geophys. Geosyst.* 9, a–n. doi:10.1029/2008GC001965

Beiki, M. (2010). Analytic Signals of Gravity Gradient Tensor and Their Application to Estimate Source Location. *GEOPHYSICS* 75, I59–I74. doi:10.1190/1.3493639

Bellahsen, N., Leroy, S., Autin, J., Razin, P., d'Acremont, E., Sloan, H., et al. (2013). Pre-existing Oblique Transfer Zones and Transfer/transform Relationships in continental Margins: New Insights from the southeastern Gulf of Aden, Socotra Island, Yemen. *Tectonophysics* 607, 32–50. doi:10.1016/j.tecto.2013.07.036

Blackman, D. K., Karson, J. A., Kelley, D. S., Cann, J. R., Früh-Green, G. L., Gee, J. S., et al. (2002). Geology of the Atlantis Massif (Mid-Atlantic Ridge, 30° N): Implications for the Evolution of an Ultramafic Oceanic Core Complex. *Mar. Geophys. Researches* 23, 443–469. doi:10.1023/B:MARI.0000018232.14085.75

Buck, W. R. (2004). Consequences of Asthenospheric Variability on Continental Rifting. in *Rheology and Deformation of the Lithosphere at Continental Margins*. Columbia University Press.

Buck, W. R., Lavier, L. L., and Poliakov, A. N. B. (2005). Modes of Faulting at Mid-ocean Ridges. *Nature* 434, 719–723. doi:10.1038/nature03358

Cande, S. C., and Kent, D. V. (1995). Revised Calibration of the Geomagnetic Polarity Timescale for the Late Cretaceous and Cenozoic. *J. Geophys. Res.* 100, 6093–6095. doi:10.1029/94jb03098

Cann, J. R., Smith, D. K., Escartin, J., and Schouten, H. (2015). Tectonic Evolution of 200 Km of Mid-Atlantic Ridge over 10 Million Years: Interplay of Volcanism and Faulting. *Geochem. Geophys. Geosyst.* 16, 2303–2321. doi:10.1002/2015GC005797

Cannat, M., Briais, A., Deplus, C., Escartin, J., Georgen, J., Lin, J., et al. (1999). Mid-Atlantic Ridge-Azores Hotspot Interactions: along-axis Migration of a Hotspot-Derived Event of Enhanced Magmatism 10 to 4 Ma Ago. *Earth Planet. Sci. Lett.* 173, 257–269. doi:10.1016/S0012-821X(99)00234-4

Cannat, M. (1993). Emplacement of Mantle Rocks in the Seafloor at Mid-ocean Ridges. *J. Geophys. Res.* 98, 4163–4172. doi:10.1029/92JB02221

Cannat, M., Mevel, C., Maia, M., Deplus, C., Durand, C., Gente, P., et al. (1995). Thin Crust, Ultramafic Exposures, and Rugged Faulting Patterns at the Mid-Atlantic Ridge (22°-24°N). *Geol.* 23, 49. doi:10.1130/0091-7613(1995)023<0049:tcuear>2.3.co;2

Cannat, M., Rommevaux-Jestin, C., and Fujimoto, H. (2003). Melt Supply Variations to a Magma-Poor Ultra-slow Spreading ridge (Southwest Indian Ridge 61° to 69°E). *Geochem. Geophys. Geosyst.* 4, 1–21. doi:10.1029/2002GC000480

Cannat, M., Sauter, D., Lavier, L., Bickert, M., Momoh, E., and Leroy, S. (2019). On Spreading Modes and Magma Supply at Slow and Ultraslow Mid-ocean Ridges. *Earth Planet. Sci. Lett.* 519, 223–233. doi:10.1016/j.epsl.2019.05.012

Combier, V., Seher, T., Singh, S. C., Crawford, W. C., Cannat, M., Escartín, J., et al. (2015). Three-dimensional Geometry of Axial Magma Chamber Roof and Faults at Lucky Strike Volcano on the Mid-Atlantic Ridge. *J. Geophys. Res. Solid Earth* 120, 5379–5400. doi:10.1002/2015JB012365

Cormier, M. H., and Sloan, H. (2019). Distinctive Seafloor Fabric Produced Near Western versus Eastern Ridge-Transform Intersections of the Northern Mid-Atlantic Ridge: Possible Influence of Ridge Migration. *Geochem. Geophys. Geosyst.* 20, 1734–1755. doi:10.1029/2018GC008101

d'Acremont, E., Leroy, S., Maia, M., Gente, P., and Autin, J. (2010). Volcanism, Jump and Propagation on the Sheba ridge, Eastern Gulf of Aden: Segmentation Evolution and Implications for Oceanic Accretion Processes. *Geophys. J. Int.* 180, 535–551. doi:10.1111/j.1365-246X.2009.04448.x

d'Acremont, E., Leroy, S., Maia, M., Patriat, P., Beslier, M.-O., Bellahsen, N., et al. (2006). Structure and Evolution of the Eastern Gulf of Aden: Insights from Magnetic and Gravity Data (Encens-Sheba MD117 Cruise). *Geophys. J. Int.* 165, 786–803. doi:10.1111/j.1365-246X.2006.02950.x

Dick, H. J. B., Lin, J., and Schouten, H. (2003). An Ultraslow-Spreading Class of Ocean ridge. *Nature* 426, 405–412. doi:10.1038/nature02128

Dick, H. J. B., Tivey, M. A., and Tucholke, B. E. (2008). Plutonic Foundation of a Slow-Spreading ridge Segment: Oceanic Core Complex at Kane Megamullion, 23°30′N, 45°20′W. *Geochem. Geophys. Geosyst.* 99, aQ05014–n. doi:10.1029/2007GC001645

Fournier, M., Chamot-Rooke, N., Petit, C., Huchon, P., Al-Kathiri, A., Audin, L., et al. (2010). Arabia-Somalia Plate Kinematics, Evolution of the Aden-Owen-Carlsberg Triple junction, and Opening of the Gulf of Aden. *J. Geophys. Res.* 115, 1–24. doi:10.1029/2008JB006257

Fournier, M., Patriat, P., and Leroy, S. (2001). Reappraisal of the Arabia-India-Somalia Triple junction Kinematics. *Earth Planet. Sci. Lett.* 189, 103–114. doi:10.1016/S0012-821X(01)00371-5

Franke, D. (2013). Rifting, Lithosphere Breakup and Volcanism: Comparison of Magma-Poor and Volcanic Rifted Margins. *Mar. Pet. Geology.* 43, 63–87. doi:10.1016/j.marpetgeo.2012.11.003

Garmany, J. (1989). Accumulations of Melt at the Base of Young Oceanic Crust. *Nature* 340, 628–632. doi:10.1038/340628a0

Hopper, J. R., Mutter, J. C., Larson, R. L., and Mutter, C. Z. (1992). Magmatism and Rift Margin Evolution: Evidence from Northwest Australia. *Geol.* 20, 853–857. doi:10.1130/0091-7613(1992)020<0853:marmee>2.3.co;2

Japsen, P. (1993). Influence of Lithology and Neogene Uplift on Seismic Velocities in Denmark: Implications for Depth Conversion of Maps. *AAPG Bull.* 77, 194–211.

Klingele, E. E., Marson, I., and Kahle, H.-G. (1991). Automatic Interpretation of Gravity Gradiometric Data in Two Dimensions: Vertical Gradient1. *Geophys. Prospect* 39, 407–434. doi:10.1111/j.1365-2478.1991.tb00319.x

Leroy, S., d'Acremont, E., Tiberi, C., Basuyau, C., Autin, J., Lucazeau, F., et al. (2010b). Recent off-axis Volcanism in the Eastern Gulf of Aden: Implications for Plume-ridge Interaction. *Earth Planet. Sci. Lett.* 293, 140–153. doi:10.1016/j.epsl.2010.02.036

Leroy, S. (2006). *ENCENS Cruise*. Paris: RV L'Atalante. doi:10.17600/6010030

Leroy, S., Gente, P., Fournier, M., d'Acremont, E., Patriat, P., Beslier, M.-O., et al. (2004). From Rifting to Spreading in the Eastern Gulf of Aden: a Geophysical Survey of a Young Oceanic basin from Margin to Margin. *Terra Nova* 16, 185–192. doi:10.1111/j.1365-3121.2004.00550.x

Leroy, S., Lucazeau, F., d'Acremont, E., Watremez, L., Autin, J., Rouzo, S., et al. (2010a). Contrasted Styles of Rifting in the Eastern Gulf of Aden: A Combined Wide-Angle, Multichannel Seismic, and Heat Flow Survey. *Geochem. Geophys. Geosyst.* 11, a–n. doi:10.1029/2009GC002963

Leroy, S. (2012). *MARGES-ADEN Cruise*. Paris: RV Beautemps-Beaupré. doi:10.17600/12090040

Leroy, S., Razin, P., Autin, J., Bache, F., d'Acremont, E., Watremez, L., et al. (2012). From Rifting to Oceanic Spreading in the Gulf of Aden: a Synthesis. *Arab J. Geosci.* 5, 859–901. doi:10.1007/s12517-011-0475-4

Lucazeau, F., and Leroy, S. (2006). *ENCENS-FLUX Cruise*. Paris: RV Le Suroît. doi:10.17600/6020080

Lucazeau, F., Leroy, S., Autin, J., Bonneville, A., Goutorbe, B., Watremez, L., et al. (2009). Post-rift Volcanism and High Heat-Flow at the Ocean-Continent Transition of the Eastern Gulf of Aden. *Terra Nova* 21, 285–292. doi:10.1111/j.1365-3121.2009.00883.x

Lucazeau, F., Leroy, S., Bonneville, A., Goutorbe, B., Rolandone, F., d'Acremont, E., et al. (2008). Persistent thermal Activity at the Eastern Gulf of Aden after continental Break-Up. *Nat. Geosci.* 1, 854–858. doi:10.1038/ngeo359

Lucazeau, F., Leroy, S., Rolandone, F., d'Acremont, E., Watremez, L., Bonneville, A., et al. (2010). Heat-flow and Hydrothermal Circulation at the Ocean-Continent Transition of the Eastern Gulf of Aden. *Earth Planet. Sci. Lett.* 295, 554–570. doi:10.1016/j.epsl.2010.04.039

MacLeod, C. J., Escartín, J., Banerji, D., Banks, G. J., Gleeson, M., Irving, D. H. B., et al. (2002). Direct Geological Evidence for Oceanic Detachment Faulting: The Mid-Atlantic Ridge, 15°45′N. *GeolGeology* 30, 879–882. doi:10.1130/0091-7613(2002)030<0879:dgefod>2.0.co;2

Marson, I., and Klingele, E. E. (1993). Advantages of Using the Vertical Gradient of Gravity for 3-D Interpretation. *GEOPHYSICS* 58, 1588–1595. doi:10.1190/1.1443374

Momoh, E., Cannat, M., and Leroy, S. (2020). Internal Structure of the Oceanic Lithosphere at a Melt-Starved Ultraslow-Spreading Mid-Ocean Ridge: Insights from 2-D Seismic Data. *Geochem. Geophys. Geosyst.* 21, e2019GC008540. doi:10.1029/2019GC008540

Momoh, E., Cannat, M., Watremez, L., Leroy, S., and Singh, S. C. (2017). Quasi-3-D Seismic Reflection Imaging and Wide-Angle Velocity Structure of Nearly Amagmatic Oceanic Lithosphere at the Ultraslow-Spreading Southwest Indian Ridge. *J. Geophys. Res. Solid Earth* 122, 9511–9533. doi:10.1002/2017JB014754

Morris, E., Detrick, R. S., Minshull, T. A., Mutter, J. C., White, R. S., Su, W., et al. (1993). Seismic Structure of Oceanic Crust in the Western North Atlantic. *J. Geophys. Res.* 98, 13879–13903. doi:10.1029/93JB00557

Mutter, J. C., and Karson, J. A. (1992). Structural Processes at Slow-Spreading Ridges. *Science* 257, 627–634. doi:10.1126/science.257.5070.627

Nonn, C., Leroy, S., Khanbari, K., and Ahmed, A. (2017). Tectono-sedimentary Evolution of the Eastern Gulf of Aden Conjugate Passive Margins: Narrowness and Asymmetry in Oblique Rifting Context. *Tectonophysics* 721, 322–348. doi:10.1016/j.tecto.2017.09.024

Nonn, C., Leroy, S., Lescanne, M., and Castilla, R. (2019). Central Gulf of Aden Conjugate Margins (Yemen-Somalia): Tectono-Sedimentary and Magmatism Evolution in Hybrid-type Margins. *Mar. Pet. Geology.* 105, 100–123. doi:10.1016/j.marpetgeo.2018.11.053

Ogg, J. G., Chen, Z.-Q., Orchard, M. J., and Jiang, H. S., 2020, Chapter 25 - the Triassic Period,Editor(s): F. M. Gradstein, J. G. Ogg, M. D. Schmitz, and G. M. Ogg, *Geologic Time Scale 2020*, Elsevier, p. 903–953. doi:10.1016/B978-0-12-824360-2.00025-5

Parsons, B., and Sclater, J. G. (19771896-1977). An Analysis of the Variation of Ocean Floor Bathymetry and Heat Flow with Age. *J. Geophys. Res.* 82, 803–827. doi:10.1029/JB082i005p00803

Patriat, P., Sloan, H., and Sauter, D. (2008). From Slow to Ultraslow: A Previously Undetected Event at the Southwest Indian Ridge at Ca. 24 Ma. *Geol.* 36 (3), 207–210. doi:10.1130/G24270A.1

Pik, R., Bellahsen, N., Leroy, S., Denèle, Y., Razin, P., Ahmed, A., et al. (2013). Structural Control of Basement Denudation during Rifting Revealed by Low-Temperature (U-Th-Sm)/He Thermochronology of the Socotra Island Basement-Southern Gulf of Aden Margin. *Tectonophysics* 607, 17–31. doi:10.1016/j.tecto.2013.07.038

Rebesco, M., Hernández-Molina, F. J., Van Rooij, D., and Wåhlin, A. (2014). Contourites and Associated Sediments Controlled by Deep-Water Circulation Processes: State-Of-The-Art and Future Considerations. *Mar. Geology.* 352, 111–154. doi:10.1016/j.margeo.2014.03.011

Robinet, J., Razin, P., Serra-Kiel, J., Gallardo-Garcia, A., Leroy, S., Roger, J., et al. (2013). The Paleogene Pre-rift to Syn-Rift Succession in the Dhofar Margin (Northeastern Gulf of Aden): Stratigraphy and Depositional Environments. *Tectonophysics* 607, 1–16. doi:10.1016/j.tecto.2013.04.017

Sandwell, D. T., and Smith, W. H. F. (2009). Global marine Gravity from Retracked Geosat and ERS-1 Altimetry: Ridge Segmentation versus Spreading Rate. *J. Geophys. Res.* 114, B01411. doi:10.1029/2008jb006008

Singh, S. C., Crawford, W. C., Carton, H., Seher, T., Combier, V., Cannat, M., et al. (2006). Discovery of a Magma Chamber and Faults beneath a Mid-Atlantic Ridge Hydrothermal Field. *Nature* 442, 1029–1032. doi:10.1038/nature05105

Sleep, N. H., and Barth, G. A. (1997). The Nature of Oceanic Lower Crust and Shallow Mantle Emplaced at Low Spreading Rates. *Tectonophysics* 279, 181–191. doi:10.1016/S0040-1951(97)00121-2

Spence, D. A., and Turcotte, D. L. (1985). Magma-driven Propagation of Cracks. *J. Geophys. Res.* 90, 575–580. doi:10.1029/JB090iB01p00575

Stein, C. A., and Cochran, J. R. (1985). The Transition between the Sheba Ridge and Owen Basin: Rifting of Old Oceanic Lithosphere. *Geophys. J. Int.* 81, 47–74. doi:10.1111/j.1365-246X.1985.tb01350.x

Thatcher, W., and Hill, D. P. (1995). A Simple Model for the Fault-Generated Morphology of Slow-Spreading Mid-oceanic Ridges. *J. Geophys. Res.* 100, 561–570. doi:10.1029/94JB02593

Tucholke, B. E., Lin, J., and Kleinrock, M. C. (1998). Megamullions and Mullion Structure Defining Oceanic Metamorphic Core Complexes on the Mid-Atlantic Ridge. *J. Geophys. Res.* 103, 9857–9866. doi:10.1029/98JB00167

Tugend, J., Gillard, M., Manatschal, G., Nirrengarten, M., Harkin, C., Epin, M.-E., et al. (2018). Reappraisal of the Magma-Rich versus Magma-Poor Rifted Margin Archetypes. *Geol. Soc. Lond. Spec. Publications* 476, 23–47. doi:10.1144/SP476.9

Watchorn, F., Nichols, G. J., and Bosence, D. W. J. (1998). "Rift-related Sedimentation and Stratigraphy, Southern Yemen (Gulf of Aden)," in *Sedimentation and Tectonics in Rift Basins Red Sea:- Gulf of Aden*. Editors B. H. Purser and D. W. J. Bosence (Dordrecht: Springer Netherlands), 165–189. doi:10.1007/978-94-011-4930-3_11

Watremez, L., Leroy, S., Rouzo, S., d'Acremont, E., Unternehr, P., Ebinger, C., et al. (2011). The Crustal Structure of the north-eastern Gulf of Aden continental Margin: Insights from Wide-Angle Seismic Data. *Geophys. J. Int.* 184, 575–594. doi:10.1111/j.1365-246X.2010.04881.x

Conflict of Interest: The authors declare that the research was conducted in the absence of any commercial or financial relationships that could be construed as a potential conflict of interest.